

On Glauber modes in Soft-Collinear Effective Theory

Christian W. Bauer

*Berkeley Center for Theoretical Physics, University of California, Berkeley, CA 94720,
Theoretical Physics Group, Lawrence Berkeley National Laboratory, Berkeley, CA 94720,
E-mail: CWBauer@lbl.gov*

Bjorn O. Lange

*Berkeley Center for Theoretical Physics, University of California, Berkeley, CA 94720,
Theoretical Physics Group, Lawrence Berkeley National Laboratory, Berkeley, CA 94720,
Theoretische Physik 1, Fachbereich Physik, Universität Siegen, D-57068 Siegen, Germany,
E-mail: B0Lange@lbl.gov*

Grigory Ovanessian

*Theoretical Division, T-2, MS B283, Los Alamos National Laboratory, Los Alamos, NM
87540,
E-mail: ovanessian@lanl.gov*

ABSTRACT: Gluon interactions involving spectator partons in collisions at hadronic machines are investigated. We find a class of examples in which a mode, called Glauber gluons, must be introduced to the effective theory for consistency.

Contents

1. Introduction	1
2. An explicit matching calculation	3
2.1 Full Theory one loop calculation	7
2.2 Conventional SCET: soft and collinear gluon exchanges	8
2.3 SCET including Glauber gluons	9
3. Pinch analysis and power counting	10
3.1 The spectator-spectator interaction in Drell-Yan	10
3.2 Relevance of Glauber gluons to other processes	14
4. Conclusions and Outlook	15

1. Introduction

Factorization underlies any theoretical prediction at hadron colliders, since it allows to separate the short distance, perturbatively calculable physics from the non-perturbative ingredients such as the parton distribution functions. First arguments in favor of factorization for hard QCD processes to all order in perturbation theory appeared over three decades ago [1, 2, 3, 4, 5]. Power counting, pinch analysis and physical pictures have been applied to analyze generic loop integrals at high energies in Refs. [6, 7], which led to the seminal work of Collins, Soper and Sterman on proofs of factorization theorems to all orders in perturbation series (see Refs. [8, 9, 10, 11] and references therein), and has been accomplished for many processes of interest. In these proofs the Landau equations [12], and their physical interpretation using the Coleman-Norton Theorem [13], were used to identify the infrared singularities giving rise to the long distance physics in arbitrary Feynman diagrams.

Singularities in Feynman diagrams arise if the integral over the loop momenta leads to pinched singularities, where the contour of the loop integration cannot be deformed to avoid the singularities in the integrands. The Coleman-Norton Theorem allows to map these pinched singularities onto configurations containing on-shell particles. For most cases, pinched singularities are due to internal propagators becoming ultrasoft or collinear to external particles, but there are also pinched singularities associated with so-called “Glauber” [14, 8] modes¹. These are internal modes which have transverse momentum much in excess of their longitudinal momentum, and can therefore not be thought of as being on the mass-shell. In particular,

¹In Ref. [8] the same momentum region was called “Coulomb”.

Glauber gluons connecting the remnants of the beams in hadronic collisions have been argued to threaten factorization [14, 15]. The presence of this transverse interaction causes significant complication in the proof of the factorization for the Drell-Yan process. However, after summing over the unobserved hadronic final states, the effects from Glauber gluons cancel, and factorization holds. This was explicitly shown to one loop order in [16] and generalized to higher orders in Refs. [17, 18]. Another approach was developed in Ref. [19], where the cancelation of Glauber gluons in the inclusive cross section was shown using the light-cone ordered perturbation theory.

Recently, a different approach to factorization proofs has emerged [20, 21, 22, 23, 24, 25, 26, 25, 27, 28, 29, 30, 31, 32, 33, 34, 35, 36, 37, 38], which is based on effective field theory techniques. Effective field theories describe the long distance physics using a limited set of degrees of freedom, with all short distance physics being integrated out of the theory and contained in the Wilson coefficients of operators. The relevant effective theory for collider physics is soft-collinear effective theory (SCET) [39, 40, 41, 42], which in its usual formulation contains collinear and ultrasoft degrees of freedom. Factorization in SCET can be shown in a very straightforward fashion, since one can show at the level of the Lagrangian that the collinear and ultrasoft degrees of freedom decouple in SCET. The advantage of the SCET approach to factorization theorems is that all long-distance ingredients of the factorization theorem are defined as matrix elements of effective theory operators, which allows to use renormalization group equations to resum large logarithms that arise in most perturbative expressions.

In its traditional formulation, SCET does not include Glauber gluons. Given their importance in traditional factorization proofs it is therefore crucial to understand if and how Glauber gluons enter the effective theory framework. An attempt to include Glauber gluons into SCET was made in [43], where the factorization of the DY cross section in the presence of a Glauber mode was reconsidered. However, there are several flaws in the arguments presented by these authors, in particular their argument about the necessity for Glauber gluons in SCET fails to consider the overlap between ultrasoft, collinear and Glauber modes. As we will show in this work, a proper treatment of this overlap is crucial to understand the contribution of Glauber gluons. Note that the inclusion of Glauber gluons into the SCET Lagrangian has also been used to describe jet broadening in dense QCD matter [44, 45].

The main purpose of this paper is to investigate whether Glauber gluons are required in SCET or not. We consider a well known operator in SCET, the operator producing two energetic back-to-back quarks, and perform the matching calculation determining its short distance Wilson coefficient using two different choices for the external states. Given that the short distance physics has to be independent of the external states, a consistent effective theory has to give the same result for both of the calculations. We will show that $\text{SCET}_{\mathcal{G}}$, the traditional formulation without Glauber modes, gives different results for different external states, while a theory that includes Glauber gluons, SCET_G , will give the correct result for both choices. This unambiguously shows that Glauber gluons need to be included for a certain class of processes. It should be pointed out, however, that Glauber gluons may be

integrated out of the effective theory, since they can not be on their mass-shell and cannot appear as external particles in perturbation theory, leading to a potential between pairs of collinear fields in opposite directions [46].

Having established the requirements of Glauber gluons in SCET_G , we will study in some more detail the relationship between pinched surfaces and the effective theory. Using a simple graphical representation of the pinched surfaces one can easily understand the necessity of Glauber gluons in the matching calculation under consideration. We then proceed to use this analysis to derive what final states are necessary to require Glauber modes to give a non-zero contribution.

The plan of the paper is as follows. In Section 2 we perform a one-loop matching calculation within SCET_G involving DY amplitude topologies and show that the effective theory breaks down, while SCET_G passes the consistency check. In Section 3 we perform the pinch analysis of a diagram with pure spectator interactions and identify the right modes of an effective theory for this process; then we discuss other processes where the Glauber mode plays a role. Finally we conclude in Section 4.

2. An explicit matching calculation

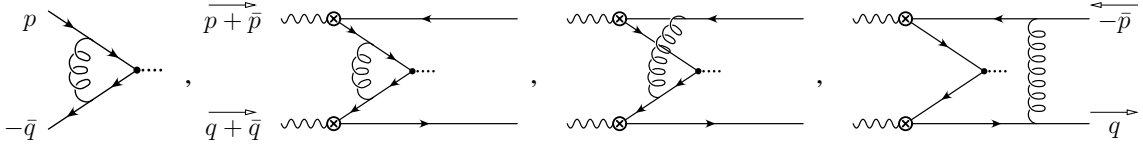


Figure 1: One-loop examples of $\langle \bar{q}q | \bar{q}\Gamma q | 0 \rangle$ (left) and $\langle \gamma^* \gamma^* | \bar{q}\Gamma q | \bar{q}q \rangle$ with active-active, spectator-active, and spectator-spectator interactions.

In this Section we will consider the well-studied SCET current $O_2 = \bar{\chi}_n \Gamma \chi_n$. The Wilson coefficient is usually calculated by an explicit calculation using partonic external states of free back-to-back quarks with large energy

$$\langle \bar{q}q | \bar{q}\Gamma q | 0 \rangle = C_2 \langle \bar{q}q | O_2 | 0 \rangle + \text{power corrections} . \quad (2.1)$$

where O_2 is built of collinear gauge invariant fields $\chi_n = W_n^\dagger \xi_n$. The Wilson line W_n contains n -collinear gluons and ξ_n is a two-component spinor describing an n -collinear quark field. (For more details see e.g. Refs [20, 21, 22, 23, 47] and References therein). The relevant Feynman diagram in the full theory is shown on the left of Fig. 1.

It is a well known consistency requirement of effective theories that the short distance Wilson coefficient of any operators has to be independent of the long distance physics in the process, and in particular it has to be independent of the external states chosen for the matching calculation. Inspired by the fact that Glauber gluons are known to manifest themselves through interactions with beam remnants, we intentionally choose more complicated external

states, namely

$$\langle \gamma^* \gamma^* | \bar{q} \Gamma q | \bar{q} q \rangle = C_2 \langle \gamma^* \gamma^* | O_2 | q \bar{q} \rangle, \quad (2.2)$$

where the two photons in the initial state and the two quarks in the final state are back-to-back with large energy. In this matrix element, each of the two off-shell photons converts into a $q\bar{q}$ pair, with a quark and an antiquark from each photon are then annihilated by the operator, while the other two quarks end up in the final state. The required Feynman diagrams in the full theory are depicted in Figure 1. We refer to the quarks that are annihilated by the operator as active, while the quarks that end up in the final state are called spectators, and divide the loop diagrams into active-active, active-spectator and spectator-spectator diagrams, as indicated in the Figure. Note that beside the internal propagators that are not involved in the loop integral, the active-active diagram is the same diagram as in the matching calculation with a $q\bar{q}$ in the initial state, and should by itself give the correct result for the matching calculation. This implies that the sum of the contributions to C_2 from active-spectator and spectator-spectator diagrams has to yield zero in a consistent effective theory.

For the purposes of this paper, i.e. identifying contributing modes, it is sufficient to study the singularity structure of the integrands, and we will therefore omit the numerator structure of propagators for simplicity. In the rest of this section we proceed as follows: The Wilson coefficient C_2 is determined via a matching calculation of the simple matrix element given in Eq. (2.1). Then we repeat the procedure for the more complicated matrix element given in Eq. (2.2). First, we will calculate the contributions to the DY process in the full theory straightforwardly. Next, we perform the matching calculation by computing the corresponding diagrams in $\text{SCET}_{\bar{Q}}$, finding that C_2 is entirely reproduced by the active-active topology, as expected. The spectator-active diagrams in $\text{SCET}_{\bar{Q}}$ match the corresponding diagrams in the full theory. In the spectator-spectator topology, however, only the soft diagram in $\text{SCET}_{\bar{Q}}$ is of leading power, and this diagram does *not* reproduce the full theory diagram. It appears that this contribution would change both the Wilson coefficient and its anomalous dimension from the findings of Eq. (2.1), which is inconsistent. Finally we consider SCET_G , which includes Glauber gluons. Repeating the matching once again, we find that Glauber gluons do not contribute for both Eq. (2.1) and the active-active part of Eq. (2.2), so that C_2 remains unchanged. Interestingly, the active-spectator topologies in the full theory and SCET_G again match identically due to the fact that the naive contribution from Glauber gluons is precisely cancelled by its overlap with the collinear gluon exchange. Finally the spectator-spectator topologies also match, and SCET_G passes the consistency check. We emphasize that the full theory diagram is identically reproduced by the sum of the soft and the Glauber gluon exchange, and not by the soft gluon exchange alone.

Before we consider the various diagrams in turn, let us set up some notation. At tree level we define

$$\langle \bar{q} q | \bar{q} \Gamma q | 0 \rangle_{\text{tree}} = \langle \bar{q} q | O_2 | 0 \rangle_{\text{tree}} = 1. \quad (2.3)$$

For the matching calculation denoted in Eq. (2.1) we denote the full theory matrix element

at one-loop by

$$\langle \bar{q}q | \bar{q}\Gamma q | 0 \rangle_{\text{loop}} = I_3, \quad (2.4)$$

where I_3 denotes the result of the 1-loop calculation. In conventional SCET $_{\bar{q}}$, the gluon is either collinear or ultrasoft (which we for brevity call soft everywhere below). They scale like $(\lambda^2, 1, \lambda)$ and $(\lambda^2, \lambda^2, \lambda^2)$ in their light-cone components, respectively, where λ is the small expansion parameter of SCET, and the light-cone components are as usual with respect to the null vectors n and \bar{n} in the $\pm z$ direction. To one loop order the amplitude for this effective theory can therefore be written as the sum of tree level and three effective theory diagrams

$$\langle \bar{q}q | O_2 | 0 \rangle = 1 + I_3^c + I_3^{\bar{c}} + I_3^s. \quad (2.5)$$

Thus, the Wilson coefficient is given by

$$C_2 = \frac{\langle \bar{q}q | \bar{q}\Gamma q | 0 \rangle}{\langle \bar{q}q | O_2 | 0 \rangle} = 1 + I_3 - (I_3^c + I_3^{\bar{c}} + I_3^s). \quad (2.6)$$

For the alternative external states, Eq. (2.2), we assign momenta $p + \bar{p}$ and $q + \bar{q}$ to the two initial virtual photons, and \bar{p} and q to the two outgoing(spectator) partons. The tree-level amplitude is simply given by the two propagators of the active quarks, such that we find in both the full and the effective theory

$$\langle \gamma^* \gamma^* | \bar{q}\Gamma q | \bar{q}q \rangle_{\text{tree}} = \langle \gamma^* \gamma^* | O_2 | \bar{q}q \rangle_{\text{tree}} = \frac{1}{p^2 \bar{q}^2}. \quad (2.7)$$

At one loop order, the full theory amplitude of the matrix element of our interest is equal to sum of three topologies, which we write as I_3 , I_4 , I_5 , namely a triangle graph in the active-active, box graphs in the spectator-active and a pentagon graph in the spectator-spectator topology. We write for the full theory calculation

$$\langle \gamma^* \gamma^* | \bar{q}\Gamma q | \bar{q}q \rangle = \frac{1}{p^2 \bar{q}^2} + \frac{1}{p^2 \bar{q}^2} I_3 + \frac{1}{\bar{q}^2} I_4^{(n)} + \frac{1}{p^2} I_4^{(\bar{n})} + I_5, \quad (2.8)$$

where the prefactors of $1/p^2$, $1/\bar{q}^2$ take into account the propagators that are independent of the loop-momenta. The (n) and (\bar{n}) superscript on the I_4 denote if the active quark is in the n or \bar{n} direction. Note that the I_3 denotes exactly the same integral as in Eq. (2.4).

In conventional SCET $_{\bar{q}}$ the one loop amplitude can be written as

$$\langle \gamma^* \gamma^* | O_2 | \bar{q}q \rangle = \frac{1}{p^2 \bar{q}^2} + \frac{1}{p^2 \bar{q}^2} (I_3^c + I_3^{\bar{c}} + I_3^s) + \frac{1}{\bar{q}^2} (I_4^{(n)c} + I_4^{(n)s}) + \frac{1}{p^2} (I_4^{(\bar{n})\bar{c}} + I_4^{(\bar{n})s}) + I_5^s, \quad (2.9)$$

where the additional superscript c , \bar{c} and s on the integrals denotes if the gluon is collinear in the n direction, collinear in the \bar{n} direction or soft. Note that we have already used the fact that some graphs, i.e. $I_4^{(n)\bar{c}}$, $I_4^{(\bar{n})c}$, I_5^c , $I_5^{\bar{c}}$, are power-suppressed. The Wilson coefficient is therefore

$$C_2 = 1 + I_3 - (I_3^c + I_3^{\bar{c}} + I_3^s) + p^2 \left[I_4^{(n)} - \left(I_4^{(n)c} + I_4^{(n)s} \right) \right] + \bar{q}^2 \left[I_4^{(\bar{n})} - \left(I_4^{(\bar{n})\bar{c}} + I_4^{(\bar{n})s} \right) \right] + p^2 \bar{q}^2 [I_5 - I_5^s]. \quad (2.10)$$

In theory SCET_G, which adds Glauber gluons with momentum scaling $(\lambda^2, \lambda^2, \lambda)$ to the conventional SCET_Q, there are new Feynman diagrams present at one loop. Denoting the triangle, box and pentagon diagrams with Glauber gluons in the loop by I_3^g , $I_4^{(n)g}$, $I_4^{(\bar{n})g}$ and I_5^g , respectively, we can write

$$\begin{aligned} \langle \gamma^* \gamma^* | O_2 | \bar{q} q \rangle_G &= \frac{1}{p^2 \bar{q}^2} + \frac{1}{p^2 \bar{q}^2} (I_3^{c'} + I_3^{\bar{c}'} + I_3^s + I_3^g) + \frac{1}{\bar{q}^2} (I_4^{(n)c'} + I_4^{(n)s} + I_4^{(n)g}) \\ &\quad + \frac{1}{p^2} (I_4^{(\bar{n})c'} + I_4^{(\bar{n})s} + I_4^{(\bar{n})g}) + I_5^s + I_5^g, \end{aligned} \quad (2.11)$$

such that we can write

$$\begin{aligned} C_2 &= 1 + I_3 - (I_3^{c'} + I_3^{\bar{c}'} + I_3^s + I_3^g) + p^2 \left[I_4^{(n)} - \left(I_4^{(n)c'} + I_4^{(n)s} + I_4^{(n)g} \right) \right] \\ &\quad + \bar{q}^2 \left[I_4^{(\bar{n})} - \left(I_4^{(\bar{n})c'} + I_4^{(\bar{n})s} + I_4^{(\bar{n})g} \right) \right] + p^2 \bar{q}^2 [I_5 - (I_5^s + I_5^g)]. \end{aligned} \quad (2.12)$$

Thus, the condition that the Wilson coefficient C_2 has to be independent of the external states chosen allows us to determine if the theory with or without Glauber gluons is correct. If SCET_Q were correct one would find

$$p^2 \left[I_4^{(n)} - \left(I_4^{(n)c} + I_4^{(n)s} \right) \right] + \bar{q}^2 \left[I_4^{(\bar{n})} - \left(I_4^{(\bar{n})\bar{c}} + I_4^{(\bar{n})s} \right) \right] + p^2 \bar{q}^2 [I_5 - I_5^s] = 0, \quad (2.13)$$

while the presence of Glauber gluons changes this condition to

$$\begin{aligned} p^2 \left[I_4^{(n)} - \left(I_4^{(n)c'} + I_4^{(n)s} + I_4^{(n)g} \right) \right] + \bar{q}^2 \left[I_4^{(\bar{n})} - \left(I_4^{(\bar{n})\bar{c}'} + I_4^{(\bar{n})s} + I_4^{(\bar{n})g} \right) \right] \\ + p^2 \bar{q}^2 [I_5 - (I_5^s + I_5^g)] = 0. \end{aligned} \quad (2.14)$$

We will explicitly show below that SCET_Q does not satisfy its consistency check Eq. (2.13), while the effective theory which contains Glauber gluons does satisfy Eq. (2.14). We will see that this difference between SCET_Q and SCET_G happens only in the spectator-spectator topology, i.e. in the last terms of Eq. (2.13) and Eq. (2.14).

It is important to note that the collinear integrals differ between the two different versions of SCET. It is well known that care has to be taken when defining the contributions arising from collinear gluons, since the various modes in the effective theory have overlap regions which can lead to double counting. When integrating over collinear loop momenta in SCET_Q, part of the integration is over a region in which the collinear momenta become soft. This would double count the soft region and therefore has to be removed from the collinear diagrams. This procedure is called “zero-bin subtraction”[48], and the collinear contributions in Eqs. (2.10) and (2.12) are all zero-bin subtracted. In particular we have

$$I_k^c = \tilde{I}_k^c - (I_k^c)_{0s}, \quad I_k^{\bar{c}} = \tilde{I}_k^{\bar{c}} - (I_k^{\bar{c}})_{0s}, \quad (2.15)$$

where \tilde{I}_k^c denotes the naive unsubtracted integrals. When adding Glauber gluons, there are more overlapping regions, requiring a more involved zero bin subtraction. We can write

$$\begin{aligned} I_k^{c'} &= \tilde{I}_k^c - \left[(I_k^{c'})_{0g} + (I_k^{c'})_{0s} - (I_k^{c'})_{0g0s} \right], \\ I_k^{\bar{c}'} &= \tilde{I}_k^{\bar{c}} - \left[(I_k^{\bar{c}'})_{0g} + (I_k^{\bar{c}'})_{0s} - (I_k^{\bar{c}'})_{0g0s} \right], \\ I_k^g &= \tilde{I}_k^g - (I_k^g)_{0s}. \end{aligned} \quad (2.16)$$

2.1 Full Theory one loop calculation

The active-active topology giving rise to I_3 in the full theory is simply a standard scalar triangle integral. In $d = 4 - 2\epsilon$ dimensions one finds²

$$I_3 = (-i)g^2\mu^{2\epsilon} \int \frac{d^d l}{(2\pi)^d} \frac{1}{[l^2 + i0] [(l+p)^2 + i0] [(l-\bar{q})^2 + i0]} \quad (2.17)$$

$$= \frac{\alpha_s}{4\pi} \frac{1}{p^+ \bar{q}^-} \left(\frac{\pi^2}{3} + \ln \frac{p^2}{p^+ \bar{q}^-} \ln \frac{\bar{q}^2}{p^+ \bar{q}^-} \right) + \mathcal{O}(\epsilon, \lambda^2). \quad (2.18)$$

The spectator-active topology can be written as the box integral

$$I_4^{(n)} = (-i)g^2\mu^{2\epsilon} \int \frac{d^d l}{(2\pi)^d} \frac{1}{[l^2 + i0] [(l-\bar{p})^2 + i0] [(l+p)^2 + i0] [(l-\bar{q})^2 + i0]} \quad (2.19)$$

$$\begin{aligned} &= \frac{\alpha_s}{4\pi} \frac{1}{\bar{q}^-} \frac{1}{\bar{p}^2 p^+ + p^2 \bar{p}^+} \left\{ \frac{\pi^2}{3} - 2 \text{Li}_2 \left(-\frac{p^2 \bar{p}^+}{\bar{p}^2 p^+} \right) \right. \\ &\quad \left. + \left[\ln \left(\frac{\bar{p}^2 p^+}{p^2 \bar{p}^+} \right) - i\pi \right] \ln \left(\frac{\bar{q}^- (p^+ \bar{p}^2 + \bar{p}^+ p^2)^2}{q^2 (p+\bar{p})^2 p^+ p^2} \right) \right\} + \mathcal{O}(\epsilon, \lambda^0). \end{aligned} \quad (2.20)$$

An analogous expression is valid for the second spectator-active integral $I_4^{(\bar{n})}$.

The spectator-spectator topology giving rise to I_5 in the full theory can be calculated via a pentagon integral which by standard procedures can be reduced to sum of five box integrals. The result is³

$$\begin{aligned} I_5 &= (-i)g^2\mu^{2\epsilon} \int \frac{d^d l}{(2\pi)^d} \frac{1}{[l^2 + i0] [(l-\bar{p})^2 + i0] [(l+p)^2 + i0] [(l-\bar{q})^2 + i0] [(l+q)^2 + i0]} \\ &= \frac{\alpha_s}{4\pi} M^+ M^- \left\{ \frac{1}{p^+ \bar{p}^+ (p+\bar{p})^2 q^- \bar{q}^- (q+\bar{q})^2} \left[\ln \frac{\bar{p}^+ p^2}{p^+ \bar{p}^2} \ln \frac{q^- \bar{q}^2}{\bar{q}^- q^2} \right. \right. \\ &\quad \left. \left. + i\pi \ln \frac{\bar{p}^2 p^2 \bar{q}^2 q^2}{\bar{p}^+ p^+ \bar{q}^- q^- (M^+ M^-)^2} + \pi^2 \right] + \frac{2\pi i}{p^+ \bar{p}^+ (p+\bar{p})^2 (M^-)^2 - q^- \bar{q}^- (q+\bar{q})^2 (M^+)^2} \right. \\ &\quad \left. \times \left[\frac{(M^-)^2 \ln \frac{M^+ (M^-)^3}{q^- \bar{q}^- (q+\bar{q})^2}}{q^- \bar{q}^- (q+\bar{q})^2} - \frac{(M^+)^2 \ln \frac{(M^+)^3 M^-}{p^+ \bar{p}^+ (p+\bar{p})^2}}{p^+ \bar{p}^+ (p+\bar{p})^2} \right] \right\} + \mathcal{O}\left(\epsilon, \frac{1}{\lambda^2}\right), \end{aligned} \quad (2.21)$$

²In all diagrams in this paper we assumed that off-shellness is positive: $p^2, \bar{p}^2, q^2, \bar{q}^2, (p+\bar{p})^2, (q+\bar{q})^2 > 0$.

³This pentagon loop integral and also integrals $I_5^g, I_4^{(n)g}, (I_4^{(n)c'})_{0g}$ have been calculated for a simplified case of “ \perp ”-less kinematics: $\mathbf{p}_\perp = \bar{\mathbf{p}}_\perp = \mathbf{q}_\perp = \bar{\mathbf{q}}_\perp = \mathbf{0}$. Since we are free to choose any external states in the matching calculation we can easily achieve these conditions.

where we have defined

$$M^+ = p^+ + \bar{p}^+, \quad M^- = q^- + \bar{q}^-. \quad (2.22)$$

To determine the Wilson coefficient C_2 we need to subtract the effective field theory diagrams from this result, which should cancel all IR divergences and reproduce the scalar one-loop result

$$C_2 = 1 + \frac{\alpha_s}{4\pi} \left[\frac{1}{\epsilon^2} + \frac{\ln \frac{\mu^2}{p^+ \bar{q}^-} + i\pi}{\epsilon} + \frac{1}{2} \ln^2 \frac{\mu^2}{p^+ \bar{q}^-} + i\pi \ln \frac{\mu^2}{p^+ \bar{q}^-} - \frac{7}{12} \pi^2 \right]. \quad (2.23)$$

2.2 Conventional SCET: soft and collinear gluon exchanges

The loop integrals for the effective theory modes in each topology can be found trivially by expanding the integrands in the full theory with the appropriate scaling of the gluon momenta before integrating over the loop momentum. The zero-bin subtraction integrals can be found similarly by expanding the effective theory loop integrals with the scaling of the overlap mode. All zero-bin integrals are scaleless in this effective theory, so they just convert infrared poles into the ultraviolet ones.

The results for all diagrams in SCET_G are given by

$$\begin{aligned} I_3^c &= \frac{\alpha_s}{4\pi} \frac{1}{p^+ \bar{q}^-} \left[-\frac{1}{\epsilon^2} - \frac{\ln \frac{\mu^2}{p^2} + i\pi}{\epsilon} - \frac{1}{2} \left(\ln \frac{\mu^2}{p^2} + i\pi \right)^2 + \frac{\pi^2}{12} \right], \\ I_3^{\bar{c}} &= \frac{\alpha_s}{4\pi} \frac{1}{p^+ \bar{q}^-} \left[-\frac{1}{\epsilon^2} - \frac{\ln \frac{\mu^2}{\bar{q}^2} + i\pi}{\epsilon} - \frac{1}{2} \left(\ln \frac{\mu^2}{\bar{q}^2} + i\pi \right)^2 + \frac{\pi^2}{12} \right], \\ I_3^s &= \frac{\alpha_s}{4\pi} \frac{1}{p^+ \bar{q}^-} \left[\frac{1}{\epsilon^2} + \frac{1}{\epsilon} \ln \frac{\mu^2 p^+ \bar{q}^-}{p^2 \bar{q}^2} + \frac{i\pi}{\epsilon} + \frac{1}{2} \ln^2 \frac{\mu^2 p^+ \bar{q}^-}{p^2 \bar{q}^2} + i\pi \ln \frac{\mu^2 p^+ \bar{q}^-}{p^2 \bar{q}^2} - \frac{\pi^2}{4} \right], \\ I_4^{(n)c} &= \frac{\alpha_s}{4\pi} \frac{1}{\bar{q}^-} \cdot \frac{1}{\bar{p}^2 p^+ + p^2 \bar{p}^+} \left\{ \frac{\ln \frac{p^2 \bar{p}^+}{\bar{p}^2 p^+} + i\pi}{\epsilon} - \frac{7\pi^2}{6} - 2 \text{Li}_2 \left(-\frac{p^2 \bar{p}^+}{\bar{p}^2 p^+} \right) \right. \\ &\quad \left. + i\pi \ln \frac{\mu^2 p^2 (p + \bar{p})^2 (\bar{p}^+)^2}{(\bar{p}^2 p^+ + p^2 \bar{p}^+)^2 \bar{p}^2} + \ln \frac{\bar{p}^2 p^+}{p^2 \bar{p}^+} \left[\ln \frac{(\bar{p}^2 p^+ + p^2 \bar{p}^+)^2}{(p + \bar{p})^2 p^+ \bar{p}^+ \bar{p}^2} - \frac{1}{2} \ln \frac{\mu^4 p^+}{p^2 \bar{p}^2 \bar{p}^+} \right] \right\}, \\ I_4^{(n)s} &= \frac{\alpha_s}{4\pi} \frac{1}{\bar{q}^-} \cdot \frac{1}{\bar{p}^2 p^+ + p^2 \bar{p}^+} \left[-\frac{\ln \frac{p^2 \bar{p}^+}{\bar{p}^2 p^+} + i\pi}{\epsilon} + \frac{1}{2} \ln \frac{\bar{p}^2 p^+}{p^2 \bar{p}^+} \ln \frac{\mu^4 p^+ \bar{p}^+ (\bar{q}^-)^2}{p^2 \bar{p}^2 (\bar{q}^2)^2} \right. \\ &\quad \left. - i\pi \ln \frac{\mu^2 p^2 (\bar{p}^+)^2 \bar{q}^-}{\bar{q}^2 (\bar{p}^2)^2 p^+} + \frac{3}{2} \pi^2 \right], \\ I_5^s &= \frac{\alpha_s}{4\pi} \frac{M^+ M^-}{p^+ \bar{p}^+ (p + \bar{p})^2 q^- \bar{q}^- (q + \bar{q})^2} \left[-\frac{2i\pi}{\epsilon} + \ln \frac{\bar{p}^+ p^2}{p^+ \bar{p}^2} \ln \left(\frac{q^- \bar{q}^2}{\bar{q}^- q^2} \right) \right. \\ &\quad \left. + i\pi \ln \left(\frac{\bar{p}^2 p^2 \bar{q}^2 q^2}{\bar{p}^+ p^+ \bar{q}^- q^- \mu^4} \right) + 3\pi^2 \right]. \end{aligned} \quad (2.24)$$

We can combine the results from the full theory and SCET_Q calculation to find

$$\begin{aligned}
I_3 - I_3^s - I_3^c - I_3^{\bar{c}} &= \frac{\alpha_s}{4\pi} \left[\frac{1}{\epsilon^2} + \frac{\ln \frac{\mu^2}{p^+ \bar{q}^-} + i\pi}{\epsilon} + \frac{1}{2} \ln^2 \frac{\mu^2}{p^+ \bar{q}^-} + i\pi \ln \frac{\mu^2}{p^+ \bar{q}^-} - \frac{7}{12} \pi^2 \right], \\
p^2 (I_4 - I_4^{(n)s} - I_4^{(n)c}) &= 0, \\
p^2 \bar{q}^2 (I_5 - I_5^s) &= \frac{\alpha_s M^+ M^-}{4\pi} \left\{ \frac{p^2 \bar{q}^2}{p^+ \bar{p}^+ (p + \bar{p})^2 q^- \bar{q}^- (q + \bar{q})^2} \left[\frac{2\pi i}{\epsilon} - 2\pi^2 + 2\pi i \ln \frac{\mu^2}{M^+ M^-} \right] \right. \\
&\quad + \frac{2\pi i p^2 \bar{q}^2}{p^+ \bar{p}^+ (p + \bar{p})^2 (M^-)^2 - q^- \bar{q}^- (q + \bar{q})^2 (M^+)^2} \\
&\quad \times \left[(M^-)^2 \frac{\ln \frac{(M^-)^3 M^+}{q^- \bar{q}^- (q + \bar{q})^2}}{q^- \bar{q}^- (q + \bar{q})^2} - (M^+)^2 \frac{\ln \frac{(M^+)^3 M^-}{p^+ \bar{p}^+ (p + \bar{p})^2}}{p^+ \bar{p}^+ (p + \bar{p})^2} \right] \Bigg\}. \tag{2.25}
\end{aligned}$$

As discussed before, the triangle diagrams are the same as with the $q\bar{q}$ external state, such that the combination $I_3 - I_3^s - I_3^c - I_3^{\bar{c}}$ reproduces the known Wilson coefficient. While the box diagrams are the same in the full and effective theory and therefore the combination $I_4 - I_4^{(n)s} - I_4^{(n)c}$ is equal to zero, this is not true for the combination $I_5 - I_5^s$. This implies that the Wilson coefficient C_2 is different when calculated with the two off-shell photons in the initial state, which shows clearly that SCET_Q does not reproduce the infrared physics of the full theory. On top of that, we can see that the combination $I_5 - I_5^s$ is UV divergent as well, indicating another failure of SCET_Q.

2.3 SCET including Glauber gluons

Having found a serious problem in SCET_Q we now repeat our matching calculation including Glauber gluons. One interesting aspect of this theory is there exists a zero-bin contribution in the spectator-active topology that does not vanish, such that it is more than merely a “pull-up” contribution [48]. The non-vanishing overlap is

$$(I_4^{(n)c'})_{0g} = \frac{\alpha_s}{4\pi} \frac{1}{\bar{q}^-} \frac{1}{\bar{p}^+ p^2 + p^+ \bar{p}^2} \left[\frac{i\pi}{\epsilon} - i\pi \ln \left(-\frac{\bar{p}^+ p^2 + p^+ \bar{p}^2}{\mu^2 (p^+ + \bar{p}^+)} - i0 \right) \right]. \tag{2.26}$$

Continuing with the calculation of the other contributions, we find that several of the integrals are either equivalent to the SCET_Q case or zero

$$I_3^{c'} = I_3^c, \quad I_3^{\bar{c}'} = I_3^{\bar{c}}, \quad I_3^g = 0. \tag{2.27}$$

For the remaining integrals we find

$$\begin{aligned}
I_4^{(n)c'} &= I_4^{(n)c} - (I_4^{(n)c'})_{0g}, \\
I_4^{(n)g} &= (I_4^{(n)c'})_{0g}, \\
I_5^g &= \frac{\alpha_s}{4\pi} \left\{ \frac{M^+ M^-}{p^+ \bar{p}^+ (p + \bar{p})^2 q^- \bar{q}^- (q + \bar{q})^2} \left[\frac{2\pi i}{\epsilon} - 2\pi^2 + 2\pi i \ln \frac{\mu^2}{M^+ M^-} \right] \right. \\
&\quad + \frac{2\pi i M^+ M^-}{p^+ \bar{p}^+ (p + \bar{p})^2 (M^-)^2 - q^- \bar{q}^- (q + \bar{q})^2 (M^+)^2} \\
&\quad \times \left[(M^-)^2 \frac{\ln \frac{(M^-)^3 M^+}{q^- \bar{q}^- (q + \bar{q})^2}}{q^- \bar{q}^- (q + \bar{q})^2} - (M^+)^2 \frac{\ln \frac{(M^+)^3 M^-}{p^+ \bar{p}^+ (p + \bar{p})^2}}{p^+ \bar{p}^+ (p + \bar{p})^2} \right] \Big\}. \quad (2.28)
\end{aligned}$$

The corresponding contributions to the Wilson coefficient C_2 from different topologies are equal to

$$\begin{aligned}
I_3 - I_3^{c'} - I_3^{\bar{c}'} - I_3^g - I_3^s &= \frac{\alpha_s}{4\pi} \left[\frac{1}{\epsilon^2} + \frac{\ln \frac{\mu^2}{p^+ \bar{q}^-} + i\pi}{\epsilon} + \frac{1}{2} \ln^2 \frac{\mu^2}{p^+ \bar{q}^-} + i\pi \ln \frac{\mu^2}{p^+ \bar{q}^-} - \frac{7}{12} \pi^2 \right], \\
p^2 \left(I_4 - I_4^{(n)c'} - I_4^{(n)g} - I_4^{(n)s} \right) &= 0, \\
p^2 \bar{q}^2 (I_5 - I_5^s - I_5^g) &= 0. \quad (2.29)
\end{aligned}$$

Thus, SCET_G with the inclusion of Glauber gluons does reproduce the correct Wilson coefficient, which can be taken as a strong indication that it is the correct effective theory.

3. Pinch analysis and power counting

3.1 The spectator-spectator interaction in Drell-Yan

As we showed in the previous Section, the spectator-spectator contribution required a Glauber gluon for the effective theory to reproduce the full theory result. In this Section we will investigate the structure of this contribution in more detail in order to get more insight into the required modes. The scalar integral contributing to the spectator-spectator diagram is given by

$$I_5 = (-i) \int \frac{d^4 l}{(2\pi)^4} \frac{1}{l^2 + i0} \frac{1}{(l + p)^2 + i0} \frac{1}{(l - \bar{p})^2 + i0} \frac{1}{(l + q)^2 + i0} \frac{1}{(l - \bar{q})^2 + i0}. \quad (3.1)$$

Decomposing the loop momentum l into its light-cone components we arrive at the following form, which is suitable for first integrating over the $+$ component by contours and leaving the \perp components as a final integration:

$$I_5 = (-i) \frac{1}{2} \int \frac{d^2 l_\perp}{(2\pi)^2} \int \frac{dl^-}{2\pi} N^-(l^-) \int \frac{dl^+}{2\pi} \prod_{i=0}^4 \frac{1}{l^+ - z_i(l^-, l_\perp)}, \quad (3.2)$$

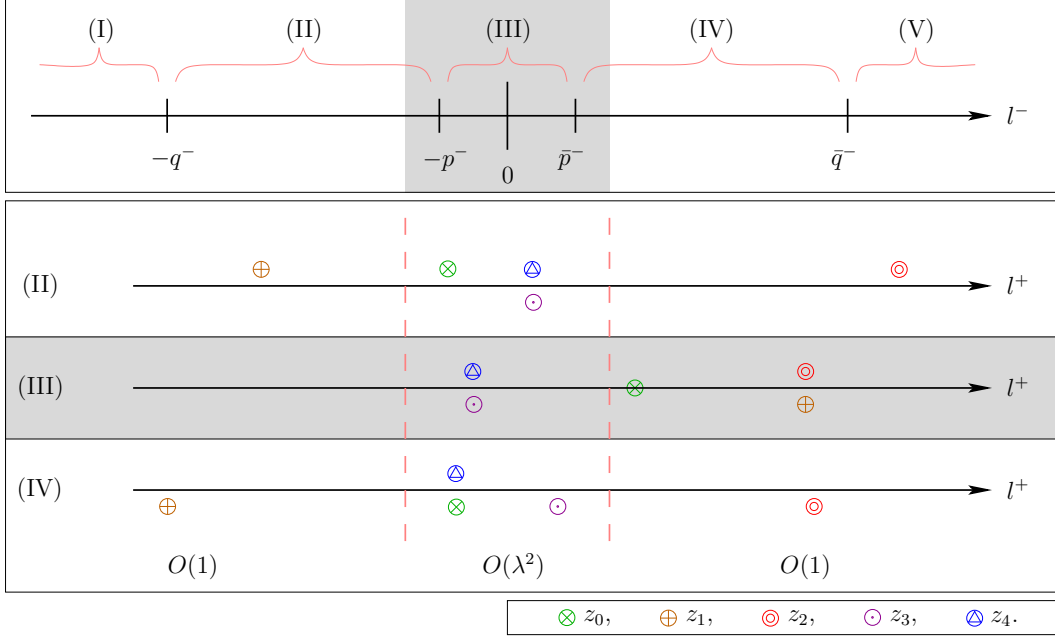


Figure 2: A few representative “constellations” of singularities during the integration over l_\perp . We show the three non-trivial intervals in l^- (regions (II), (III), (IV) above) and one sample projection onto the complex l^+ plane for each region. The poles in the complex l^+ plane can be pinched in different locations, depending on the values of l^- and l_\perp . For example, in region (III) l^- counts as $O(\lambda^2)$, and there are two pinched singularities: first, there exists a value of l_\perp for which l^+ is pinched between z_3 and $z_4 \sim O(\lambda^2)$; second, there exists a (generally different) value of l_\perp for which l^+ is pinched between z_1 and $z_2 \sim O(1)$.

where $[N^-(l^-)]^{-1} = l^-(l^- + p^-)(l^- - \bar{p}^-)(l^- + q^-)(l^- - \bar{q}^-)$. The positions of the singularities z_i in the complex l^+ plane are functions of l^- and l_\perp , as well as the external momentum components. Explicitly they are given by

$$\begin{aligned}
 z_0(l^-, l_\perp) &= \frac{l_\perp^2 - i0}{l^-}, \\
 z_1(l^-, l_\perp) &= \frac{(l_\perp + p_\perp)^2 - i0}{l^- + p^-} - p^+, \quad z_3(l^-, l_\perp) = \frac{(l_\perp + q_\perp)^2 - i0}{l^- + q^-} - q^+, \\
 z_2(l^-, l_\perp) &= \frac{(l_\perp - \bar{p}_\perp)^2 - i0}{l^- - \bar{p}^-} + \bar{p}^+, \quad z_4(l^-, l_\perp) = \frac{(l_\perp - \bar{q}_\perp)^2 - i0}{l^- - \bar{q}^-} + \bar{q}^+. \quad (3.3)
 \end{aligned}$$

Note that the locations of the poles above or below the real axis changes during the integration over l^- at the transitions $l^- = -q^- \sim \mathcal{O}(1)$, $\bar{q}^- \sim \mathcal{O}(1)$, $-p^- \sim \mathcal{O}(\lambda^2)$, $\bar{p}^- \sim \mathcal{O}(\lambda^2)$ and $l^- = 0$. For $l^- < -q^-$ or $l^- > \bar{q}^-$, all poles are either above or below the real axis, such that the total integral vanishes. We can divide the remaining range of l^- into three regions $-q^- < l^- < -p^-$, $-p^- < l^- < \bar{p}^-$ and $p^- < l^- < \bar{q}^-$, as depicted schematically in Figure 2.

We begin by considering the region $-p^- < l^- < \bar{p}^-$, labeled (III) in the Figure. In this

case the poles in z_1 and z_3 are below the real axis, while the poles in z_2 and z_4 are above the real axis. The pole in z_0 is either above or below the real axis⁴, depending on the sign of l^- .

Since $l^- \sim O(\lambda^2)$ the pole location z_i , and hence the magnitude of l^+ after its residue is taken, depends only on the size of l_\perp . In particular, $z_0 \sim O(l_\perp^2/\lambda^2)$ depends strongly on the power assignment of l_\perp , which demonstrates the shortcomings of the cartoon in Figure 2. We find that a new approach to illustrate the l_\perp dependence is in order, which we present in Fig. 3.

The top left part of Fig. 3 shows the magnitude of the pole position z_i as a function of l_\perp on a double logarithmic scale. The green, orange, red, magenta and blue curves correspond to z_0, z_1, z_2, z_3 and z_4 , respectively. We also visualize the sign of the pole by showing the z_i above the real axis by solid lines, those with poles below the axis by dashed lines, and z_0 , whose pole that can change location, by the dot-dashed line. Whenever a solid and a dashed line are present at the same point, the two corresponding poles can be pinched. For example, for $l_\perp \sim O(\lambda)$ there is a pinch between z_3 and z_4 leading to $l^+ \sim \lambda^2$, but also a pinch between z_0, z_1 and z_2 leading to $l^+ \sim 1$.

Next, for a given l_\perp , we can also determine the magnitude of the contribution of each of the residues to the integrand of I_5 . In the top right part of Fig. 3 we illustrate the magnitude of the integral, taking into account the scaling of the d^4l . In this Figure we have chosen to close the contour above the real axis, so that the poles below the real axis do not contribute. Note that leading power corresponds to λ^{-4} , consistent with Eq. (2.8).

These diagrams can be used to identify the modes required in an effective theory. From the top right plot we see that a leading order contribution λ^{-4} can only come from the residue of z_4 , and that l_\perp has to be between λ and λ^2 . The residue from z_2 always leads to a power suppressed contribution, in agreement with the explicit calculation performed in the previous Section. From the top left plot we see that the corresponding poles are indeed pinched and we also read off that for these cases the momentum component l^+ scales as λ^2 . Thus, the two scalings of the loop momentum that give rise to leading order effects in the spectator-spectator contribution are

$$l^\mu \sim (\lambda^2, \lambda^2, \lambda^2), \quad \text{and} \quad l^\mu \sim (\lambda^2, \lambda^2, \lambda), \quad (3.4)$$

which are the soft and Glauber mode. We will come back to the possibility of l^\perp being somewhere in between λ and λ^2 later.

So far we have only considered the case $l^- \sim O(\lambda^2)$, and in particular the region $l^- \in [-p^-, \bar{p}^-]$. Outside that region one of the poles z_1, z_2 will cross the real axis onto the other half plane, unpinching a singularity, which only results in the removal of the already power-suppressed (collinear) contribution of its residue. For completeness we shall also mention that the case $l^- \sim O(1)$ will again lead to no further leading-power contributions.

It is an easy exercise to draw plots analogous to the top right plot of Figure 3 for the effective theory. As one obtains the integrals in the effective theory by expanding the full integral about the loop momentum modes, one similarly finds that the top right plot in

⁴In the Figure we chose to indicate this by placing the pole directly on the real axis.

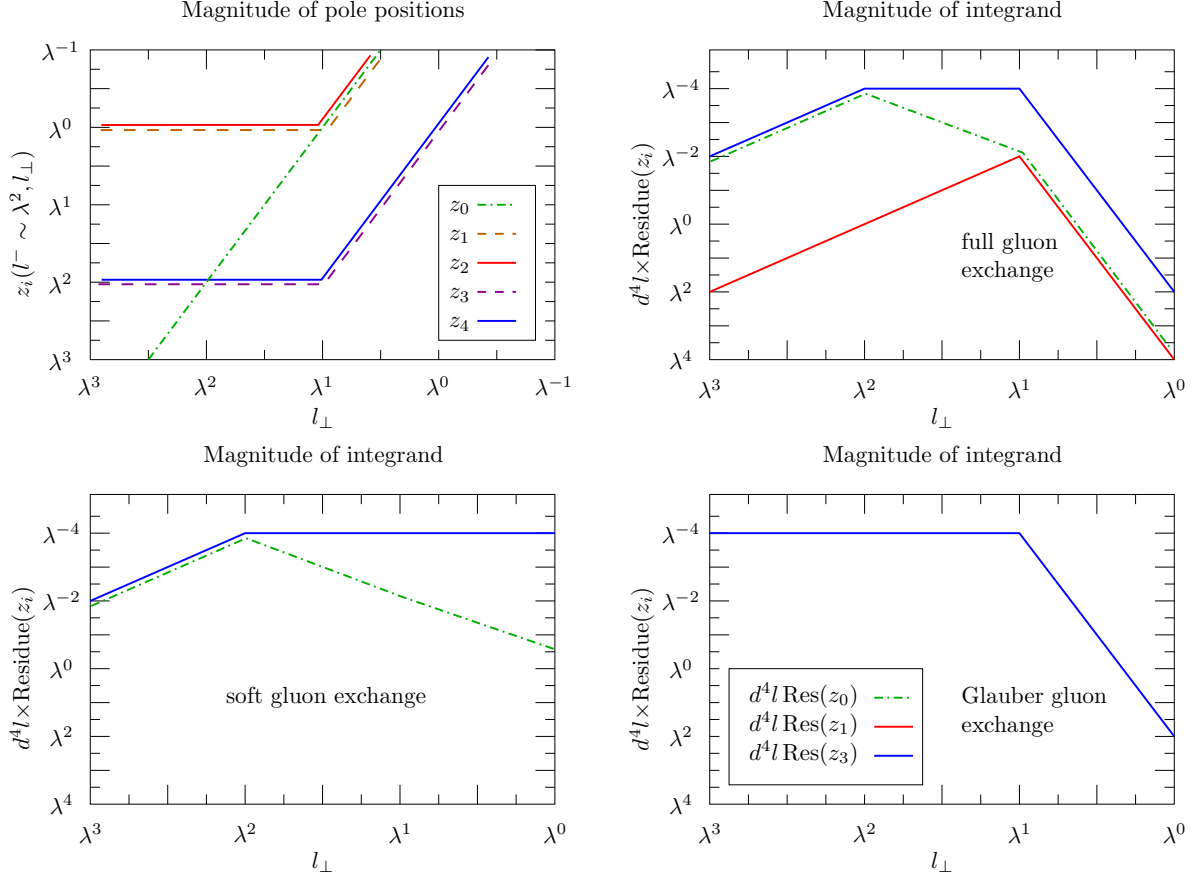


Figure 3: Top Left: magnitude of pole locations as a function of l_\perp . Dashed lines denote poles in the lower half plane, while solid ones are in the upper half plane. The dash-dotted line may be on either side. Top Right: magnitude of the residues of poles in the upper half plane (including integration measures). The color coding is identical to the one on the left. Lower Row: magnitude of the residues for the effective modes soft (left) and Glauber (right).

Figure 3 is simply expanded around the modes, which is shown in the lower row of the Figure. In this case, expanding the integrand around soft loop momentum will reproduce the plot below $l_\perp \sim O(\lambda^2)$ and continue the straight segment to the right of it indefinitely. This is shown in the lower left plot. Thus, the soft contribution reproduces the infrared region and picks up a $1/\varepsilon_{\text{UV}}$ singularity. On the other hand, an expansion around the Glauber scaling (lower right plot) will reproduce the region around $l_\perp \sim \lambda$ and pick up a $1/\varepsilon_{\text{IR}}$ pole. The overlap between those two modes is obtained by expanding the Glauber integral around the soft limit, which is a scaleless integral and provides the subtraction of both poles, thus reproducing the full theory at leading power.

In the above we have only considered the two discrete choices $l_\perp = \lambda$ or $l_\perp = \lambda^2$. However, the Figures seem to indicate that any scaling of l_\perp between these two extremes leads to a

leading order contribution and has a pinched pole. The question then arises why we do not have to consider more modes, such as one with momentum scaling as $l^\mu \sim (\lambda^2, \lambda^2, \lambda^{3/2})$. Expanding around this point, we would obtain a mode in the effective theory similar to the construction discussed above. The important point, however, is that the overlap contributions between this mode and the Glauber and soft modes are identical to the new mode itself. Thus, after taking the overlap contributions into account, the contributions from any additional modes vanish. A similar argument can be made that no additional modes are required even if power suppressed terms are considered.

3.2 Relevance of Glauber gluons to other processes

In this Section we will assume that a generic one-loop diagram has a pinch singularity in the Glauber region and derive some necessary characteristics of the diagram from this and a few other assumptions. The following analysis is closely related to the preceding Section. Previously we started by studying a loop diagram with given external leg momenta and found that the Glauber region is pinched. Here we are going the opposite way: Let us start with the assumptions that

1. the loop momentum $l \sim (\lambda^2, \lambda^2, \lambda)$ leads to a pinch singularity,
2. external momenta k_i are on the mass-shell,
3. a momentum component can be at most $O(1)$, no inverse powers of λ .

Our choice will be to perform the l^+ integration by contours. Consider the propagator $(l+k)^{-2}$, which leads to a simple pole of the form $(l^+ - z)^{-1}$ with

$$z = \frac{(l_\perp + k_\perp)^2 - i0}{l^- + k^-} - k^+. \quad (3.5)$$

We will use the following ansatz for the scaling of k , namely $k^\pm \sim O(\lambda^{n_\pm})$, $k_\perp \sim O(\lambda^{n_\perp})$. The on-shell condition means that $n_+ + n_- = 2n_\perp$. Since $l^+ \sim O(\lambda^2)$, it follows that z must also scale like $O(\lambda^2)$, and one of the following conditions (a) or (b) must be satisfied:

$$\begin{aligned} (a) \quad & 2 \min(1, n_\perp) - \min(2, n_-) = 2 \quad \text{and} \quad n_+ \geq 2, \\ (b) \quad & 2 \min(1, n_\perp) - \min(2, n_-) > 2 \quad \text{and} \quad n_+ = 2. \end{aligned}$$

It is easy to show that condition (b) can never be satisfied with the assumption that $n_\pm, n_\perp \geq 0$, and that the only scaling of k consistent with (a) is $k \sim (\lambda^2, 1, \lambda)$, i.e. collinear. Strictly speaking we get $n_- = 0$ and $n_\perp \geq 1$, e.g. $(\lambda^4, 1, \lambda^2)$ would also be allowed. The momentum with largest invariant mass, however, (the least restrictive condition) is the standard collinear one. External legs with even smaller invariant masses will pinch the loop integral also in a Glauber-type configuration, for example $l \sim (\lambda^4, \lambda^4, \lambda^2)$, which is readily rescaled by $\lambda' = \lambda^2$ to yield the same result.

We have therefore found that attaching an incoming collinear leg to the loop is consistent with a Glauber loop momentum, although certainly not sufficient. In particular, note that k^- dominates over l^- . In order to obtain a pinch singularity, we will hence need another leg with collinear scaling, but with outgoing momentum⁵. Next, we note that it was a choice to perform the l^+ integration by contour, which pins down the l^+ scaling but leaves l^- open. We therefore repeat the above argument starting with the l^- component by contours and find that we need to attach two more legs to the loop diagram, one in- and one outgoing with anti-collinear momentum scaling.

It follows that any process involving diagrams of the form depicted in Figure 4 will be sensitive to Glauber interactions. The characteristics are that there are at least four the external legs, with two of them collinear and two of them anticollinear. For a pinch singularity, each pair must consist of an incoming and an outgoing momentum. The simplest such case is forward scattering of a collinear with an anti-collinear field, where no other external legs are attached to the diagram. Multiple exchanges of Glauber gluons will give rise to an effective potential between the collinear and anti-collinear fields when integrating Glauber gluons out of the theory. This is similar to the exchange of potential gluons in non-relativistic QCD, and can be found elsewhere in the literature [49, 50]. In our case of Drell-Yan far from machine threshold there is one extra leg in the diagram from which the lepton pair will emerge. From the point of view of Glauber gluon relevance this case is identical to Higgs production, or indeed any New Physics particle production in hadronic collisions away from machine threshold.

4. Conclusions and Outlook

Using an explicit matching calculation we have investigated whether Glauber gluons are required as a degree of freedom in SCET. Focusing on the operator O_2 , whose Wilson coefficient is well known, we showed that Glauber gluons are required if the matching is performed with final states that contain both initial and final collinear particles in the same collinear direction.

Even though we did not directly consider the Drell-Yan process, our choice of external states was such that all contributions of the Drell-Yan process, namely spectator-active and spectator-spectator interactions in addition to active-active were present. This allows us to make parallels between our conclusion about the consistency of matching and the correct modes for the Drell-Yan amplitude. Our conclusion is that for the exclusive Drell-Yan amplitude the correct effective theory would require Glauber modes. Note that we have not discussed under what circumstances the contribution of Glauber gluons cancel when squaring the amplitude.

For our analysis it was important to avoid double counting between the modes by performing zero-bin subtractions [48] from the collinear and Glauber modes. It is worthwhile to

⁵The next propagator will then be $(l + K)^{-2}$ with $K = k - k'$. Since both k and k' have collinear scaling, so does K .

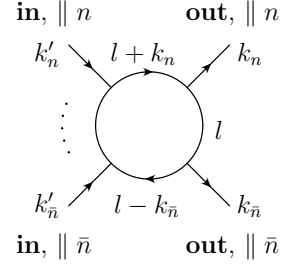


Figure 4: A one-loop diagram with loop momentum l .

emphasize the spectator-active case for SCET_G, since in this topology there is an interesting example of non-vanishing zero-bin subtraction from the naive collinear mode $(I_4^{(n)c'})_{0g} \neq 0$. It shows that taking these subtraction serious renders the effective theory robust toward the introduction of other modes and does not invalidate previous calculations.

From the scaling of the Glauber mode it is apparent that it cannot be made exactly on-shell. However in the case of the spectator-spectator topology there is a pinch singularity in the Glauber region. Thus we find an apparent contradiction to the Coleman-Norton theorem [13], which states that all pinched surfaces arise from on-shell degrees of freedom. This contradiction is resolved if one notices that Landau Equations used in the Coleman-Norton theorem are conditions for appearance of a true singularity, which correspond to the case when the loop integral is infinite, i.e when power counting parameter of the effective theory vanishes: $\lambda = 0$. In this limit both the Glauber and soft momenta are identical to each other $l_g^\mu = l_s^\mu = 0$. Of course in this limit both modes become on-shell, so the contradiction with Coleman-Norton theorem goes away.

It would be interesting to reformulate the Landau equations taking into account the proper power counting, i.e. instead of writing down a condition of having a true pinch singularity, find a condition for pinched poles to occur at distance of say order λ^2 from each other. It should be possible to use such an analysis to discover both Glauber and soft pinches in the spectator-spectator diagram directly from such relaxed Landau Equations. Understanding this question in details might potentially be of practical importance since it can lead to a nice recipe for arbitrary process on how to read off the correct long distance modes (valid to all orders in perturbation theory with a possibility to include power corrections). This, however, is beyond the scope of the present paper and will be studied elsewhere.

Another important step is to study the effect of Glauber gluons in SCET on physical observables, and not just amplitudes as done in this paper. The expectation here would be to understand the cancellation of Glauber gluons in the inclusive in the final hadronic state Drell-Yan cross-section, which was proved in full QCD in Refs. [16, 17, 18]. The main challenge in doing so is that the Glauber mode scaling is such that the corresponding particle is always off-shell, such that it can not be naively included in the SCET Lagrangian. A better way to proceed might be to interpret this mode as an effective potential, giving rise to forward scattering of two collinear particles in different directions [46].

Acknowledgments

We would like to thank Thomas Becher for helpful discussions, and Christopher Lee, Zoltan Ligeti, George Sterman and Iain Stewart for comments on the manuscript. This work was supported by the Director, Office of Science, Offices of High Energy and Nuclear Physics of the U.S. Department of Energy under the Contract DE-AC02-05CH11231. G.O. was additionally supported under the Contract DE-AC52-06NA25396 and in part by the LDRD program at LANL. B.L. would like to thank the University of Siegen for their hospitality during the final stages of this project.

References

- [1] D. Amati, R. Petronzio, and G. Veneziano *Nucl. Phys.* **B146** (1978) 29–49.
- [2] S. B. Libby and G. F. Sterman *Phys. Rev.* **D18** (1978) 3252.
- [3] A. H. Mueller *Phys. Rev.* **D18** (1978) 3705.
- [4] S. Gupta and A. H. Mueller *Phys. Rev.* **D20** (1979) 118.
- [5] R. K. Ellis, H. Georgi, M. Machacek, H. D. Politzer, and G. G. Ross *Nucl. Phys.* **B152** (1979) 285.
- [6] G. F. Sterman *Phys. Rev.* **D17** (1978) 2773.
- [7] G. F. Sterman *Phys. Rev.* **D17** (1978) 2789.
- [8] J. C. Collins and G. F. Sterman *Nucl. Phys.* **B185** (1981) 172.
- [9] J. C. Collins and D. E. Soper *Nucl. Phys.* **B193** (1981) 381.
- [10] J. C. Collins and D. E. Soper *Ann. Rev. Nucl. Part. Sci.* **37** (1987) 383–409.
- [11] J. C. Collins, D. E. Soper, and G. F. Sterman *Adv. Ser. Direct. High Energy Phys.* **5** (1988) 1–91, [[hep-ph/0409313](#)].
- [12] L. D. Landau *Nucl. Phys.* **13** (1959) 181–192.
- [13] S. Coleman and R. E. Norton *Nuovo Cim.* **38** (1965) 438–442.
- [14] G. T. Bodwin, S. J. Brodsky, and G. P. Lepage *Phys. Rev. Lett.* **47** (1981) 1799.
- [15] J. C. Collins, D. E. Soper, and G. F. Sterman *Phys. Lett.* **B109** (1982) 388.
- [16] J. C. Collins, D. E. Soper, and G. Sterman *Nucl. Phys.* **B223** (1983) 381.
- [17] G. T. Bodwin *Phys. Rev.* **D31** (1985) 2616 [Erratum: *Phys. Rev. D* 34 (Dec, 1986), 3932].
- [18] J. C. Collins, D. E. Soper, and G. F. Sterman *Nucl. Phys.* **B261** (1985) 104.
- [19] S. M. Aybat and G. F. Sterman *Phys. Lett.* **B671** (2009) 46–50, [[arXiv:0811.0246](#)].
- [20] C. W. Bauer, S. Fleming, D. Pirjol, I. Z. Rothstein, and I. W. Stewart *Phys. Rev.* **D66** (2002) 014017, [[hep-ph/0202088](#)].
- [21] C. W. Bauer, A. V. Manohar, and M. B. Wise *Phys. Rev. Lett.* **91** (2003) 122001, [[hep-ph/0212255](#)].
- [22] C. W. Bauer, C. Lee, A. V. Manohar, and M. B. Wise *Phys. Rev.* **D70** (2004) 034014, [[hep-ph/0309278](#)].
- [23] A. V. Manohar *Phys. Rev.* **D68** (2003) 114019, [[hep-ph/0309176](#)].
- [24] Y. Gao, C. S. Li, and J. J. Liu *Phys. Rev.* **D72** (2005) 114020, [[hep-ph/0501229](#)].
- [25] A. Idilbi, X.-d. Ji, and F. Yuan *Phys. Lett.* **B625** (2005) 253–263, [[hep-ph/0507196](#)].
- [26] A. Idilbi and X.-d. Ji *Phys. Rev.* **D72** (2005) 054016, [[hep-ph/0501006](#)].
- [27] J. Chay and C. Kim *Phys. Rev.* **D75** (2007) 016003, [[hep-ph/0511066](#)].
- [28] A. V. Manohar *Phys. Lett.* **B633** (2006) 729–733, [[hep-ph/0512173](#)].

- [29] T. Becher, M. Neubert, and B. D. Pecjak *JHEP* **01** (2007) 076, [[hep-ph/0607228](#)].
- [30] P.-y. Chen, A. Idilbi, and X.-d. Ji *Nucl. Phys.* **B763** (2007) 183–197, [[hep-ph/0607003](#)].
- [31] C. Lee and G. F. Sterman *Phys. Rev.* **D75** (2007) 014022, [[hep-ph/0611061](#)].
- [32] S. Fleming, A. H. Hoang, S. Mantry, and I. W. Stewart *Phys. Rev.* **D77** (2008) 074010, [[hep-ph/0703207](#)].
- [33] S. Fleming, A. H. Hoang, S. Mantry, and I. W. Stewart *Phys. Rev.* **D77** (2008) 114003, [[arXiv:0711.2079](#)].
- [34] T. Becher, M. Neubert, and G. Xu *JHEP* **07** (2008) 030, [[arXiv:0710.0680](#)].
- [35] M. D. Schwartz *Phys. Rev.* **D77** (2008) 014026, [[arXiv:0709.2709](#)].
- [36] C. W. Bauer, S. P. Fleming, C. Lee, and G. F. Sterman *Phys. Rev.* **D78** (2008) 034027, [[arXiv:0801.4569](#)].
- [37] C. W. Bauer, A. Hornig, and F. J. Tackmann *Phys. Rev.* **D79** (2009) 114013, [[arXiv:0808.2191](#)].
- [38] C. W. Bauer, N. D. Dunn, and A. Hornig [arXiv:1002.1307](#).
- [39] C. W. Bauer, S. Fleming, and M. E. Luke *Phys. Rev.* **D63** (2000) 014006, [[hep-ph/0005275](#)].
- [40] C. W. Bauer, S. Fleming, D. Pirjol, and I. W. Stewart *Phys. Rev.* **D63** (2001) 114020, [[hep-ph/0011336](#)].
- [41] C. W. Bauer and I. W. Stewart *Phys. Lett.* **B516** (2001) 134–142, [[hep-ph/0107001](#)].
- [42] C. W. Bauer, D. Pirjol, and I. W. Stewart *Phys. Rev.* **D65** (2002) 054022, [[hep-ph/0109045](#)].
- [43] F. Liu and J. P. Ma [arXiv:0802.2973](#).
- [44] A. Idilbi and A. Majumder *Phys. Rev.* **D80** (2009) 054022, [[arXiv:0808.1087](#)].
- [45] F. D’Eramo, H. Liu, and K. Rajagopal [arXiv:1006.1367](#).
- [46] I. Stewart and I. Rothstein (work in progress). Talk “Glauber Gluons in SCET” presented by I. Stewart at SCET2010 in Ringberg, Germany, 2010.
- [47] C. W. Bauer, O. Cata, and G. Ovanesyan [arXiv:0809.1099](#).
- [48] A. V. Manohar and I. W. Stewart *Phys. Rev.* **D76** (2007) 074002, [[hep-ph/0605001](#)].
- [49] A. Pineda and J. Soto *Phys. Rev.* **D59** (1999) 016005, [[hep-ph/9805424](#)].
- [50] M. E. Luke, A. V. Manohar, and I. Z. Rothstein *Phys. Rev.* **D61** (2000) 074025, [[hep-ph/9910209](#)].